EYE-CLIMA
Verifying emissions of climate forcers

# Recommendation on whether CO source of $CO_2$ needs to be accounted for in $CO_2$ inversions

## MILESTONE 3


**Author(s):** Audrey Fortems-Cheiney



**Date of submission:** 22-04-2025
**Version:** 1.0
**Responsible partner:** Science Partners
**Milestone due date:** 30-08-2024
**Dissemination level:** Public

**Call:** HORIZON-CL5-2022-D1-02
**Topic:** Climate Sciences and Responses
**Project type:** Research and Innovation Action
**Lead Beneficiary:** NILU - Norsk Institutt for Luftforskning

This project has received funding from the European Union's Horizon Europe research and innovation programme under grant agreement No 101081395

## Document History

| Version | Date | Comment | Modifications made by |
|---|---|---|---|
| 0.1 | 14-03-2025 | First Draft | Audrey Fortems-Cheiney (SP) |
| 0.2 | 21-03-2025 | Internal review | Rona Thompson (NILU) |
| 1.0 | 22-04-2025 | Submitted to Commission | Rona Thompson (NILU) |



This project has received funding from the European Union's Horizon Europe research and innovation programme under grant agreement No 101081395

## Introduction

One of the main objectives of EYE-CLIMA is to support European and national policies through its top-down emissions estimation methodology and verification of national greenhouse gas inventories (NGHGIs). There is indeed a growing interest in top-down verification methods, linking emissions to changes in atmospheric concentrations, and the use of atmospheric observations to verify NGHGIs has been highlighted in the 2019 refinement of the IPCC Guidelines. EYE-CLIMA has a strong focus on improving the accuracy of regional inversions for $CO_2$ fluxes, especially in Europe with the goal to support Europe's Green Deal policies.

Different sources of uncertainties can all interact in regional inversions, including misrepresentation of i) the a priori knowledge from fluxes, ii) initial and boundary conditions and iii) the atmospheric chemistry and transport modelling. For instance, the inversions generally do not take the atmospheric source of $CO_2$ from the oxidation of CO into account, assuming this source is negligible.

This document describes sensitivity tests performed to assess the impact of the atmospheric CO source of $CO_2$ on the $CO_2$ concentrations and on the $CO_2$ land ecosystem fluxes estimated from the inversions in the frame of the Task T3.8 of the EYECLIMA project. Such assessment has been made with simulations for the year 2019 and inversions for the month of June 2019, when the posterior estimates at the 0.5° spatial resolution identify a $CO_2$ peak uptake (Deliverable D3.1) and is presented in this deliverable.



This project has received funding from the European Union's Horizon Europe research and innovation programme under grant agreement No 101081395

# TABLE OF CONTENTS





This project has received funding from the European Union's Horizon Europe research and innovation programme under grant agreement No 101081395

# 1. Inverse modelling system and experimental framework

The inversion system relies on the coupling between the variational mode of the Community Inversion Framework (CIF, Berchet et al., 2021), the regional chemistry transport model (CTM), CHIMERE (Menut et al., 2013; Mailler et al., 2017) and the adjoint of this model (Fortems-Cheiney et al., 2021b).

## 1.1. Configuration of the regional CHIMERE chemistry-transport model for the simulation of CO and $CO_2$ over Europe

The CHIMERE domain for Europe covers latitudes 31.75-73.75°N and longitudes 15.25°W -34.75°E with a 0.5°×0.5° horizontal resolution and 17 vertical layers up to 200 hPa. Meteorological forcing for CHIMERE is generated using operational forecasts from the Integrated Forecasting System (IFS) of the European Centre for Medium Range Weather Forecasting (ECMWF).

The reference configuration used here for the inversion of the $CO_2$ land ecosystem fluxes in Europe is the one developed for the preliminary inversions documented in Deliverable D3.1 in the frame of the EYECLIMA project. Two model set-ups have been used. First, considering $CO_2$ as a passive tracer (the reference) in which only the atmospheric transport modeling components have been used (the chemistry modeling components were deactivated), and second considering $CO_2$ as a labile tracer with the chemistry modeling components activated. The chemical scheme used here is MELCHIOR-2, with more than 100 reactions, including 24 for inorganic chemistry (Lattuati, 1997; Derognat et al., 2003), describing the CO chemistry.

The different components needed for the simulations of CO and $CO_2$ are described in the following sections.

## 1.2. CO and $CO_2$ boundary conditions

Initial, lateral and top conditions for $CO_2$ concentrations at the boundaries of the model and at the simulations initial times are generated from the latest Copernicus Atmospheric Monitoring Service (CAMS) global $CO_2$ inversions (v22r1) assimilating surface data (Chevallier et al., 2005; Chevallier et al., 2010). This global inversion product is also used to complement the vertical columns of $CO_2$ above the top boundary of CHIMERE when comparing the model to $XCO_2$ observations.

Initial and boundary conditions for several key gaseous species responsible for the oxidation capacity of the lower atmosphere (e.g., CO, NO, $NO_2$, $O_3$, $H_2O_2$, HCHO, etc) were specified using monthly climatological data from LMDz-INCA global model (Szopa, 2008).

## 1.3. Estimates for the CO emissions

The CO emissions are based on the TNO-GHGco version 3, updated from the TNO inventory documented in Kuenen et al. (2014) and in Super et al. (2020), based on country emission reporting to the European Monitoring and Evaluation Program (EMEP)/Center on Emission Inventories Projection (CEIP). The TNO-GHGco-v3 inventory maps CO emissions at a 6×6 $km^2$ horizontal resolution. It combines emissions from area sources, set at the surface, and from point sources. Emissions from point sources, mainly from the energy production and the industrial sectors, are distributed on the first eight vertical model layers in CHIMERE depending on the typical injection heights provided in the TNO inventory, based on Bieser et al. (2011). In the TNO inventory, annual and national budgets are disaggregated in space based on proxies of the different sectors (Kuenen et al., 2014). Temporal disaggregation is based on temporal profiles provided per GNFR sector code with typical month to month, weekday to weekend and diurnal variations (Ebel et al., 1994, Menut et al., 2011).



This project has received funding from the European Union's Horizon Europe research and innovation programme under grant agreement No 101081395

It should be noted that CO emissions from fires and CO biogenic emissions are not considered, as in Fortems-Cheiney et al. (2023). In addition to CO, the chemical scheme MELCHIOR-2 needs emissions from other species, such as non-methane volatile organic compounds (NMVOCs). The anthropogenic emissions for NMVOCs are obtained from the EMEP inventory (Vestreng et al., 2005). The fixed biogenic NMVOC emissions are derived from the MEGAN model (Guenther et al., 2006). The different emission products have been aggregated at the 0.5°×0.5° horizontal resolution of the CHIMERE grid.

## 1.4. Prior estimates of the $CO_2$ land ecosystem fluxes and other $CO_2$ surface fluxes

The principle of the inversion is to correct *a priori* estimates of the net land ecosystem flux maps later referred as “prior" fluxes. Here, we have used the "CRUERA" prior NBP, from a European scale simulation run in the frame of the EYE-CLIMA project, with a dedicated forcing at the spatial resolution of 0.125°. This prior is described in the Deliverable D2.3 of the EYECLIMA project. We have aggregated these prior fluxes at the 0.5°x0.5° horizontal resolution of the CHIMERE grid.

The other component of $CO_2$ fluxes from ocean and anthropogenic activities are fixed throughout the inversion. We have aggregated these fluxes at the 0.5°x 0.5° horizontal resolution of the CHIMERE grid.

The anthropogenic fossil fuel and biofuel $CO_2$ emissions (Gerbig and Koch, 2023) are derived from the TNO-GHGco version 3 inventory, as for CO.

The estimate of sea/ocean fluxes within the CHIMERE domain is based on a hybrid product combining the coastal ocean flux estimates from the University of Bergen and a global ocean estimate from MPI-BGC-Jena (Rödenbeck et al., 2014; McGrath et al., 2023). The data is provided from 2005 to 2020 at a 0.125°×0.125° horizontal resolution and at daily temporal resolution.

## 1.5. Observations

The inversion assimilates the relatively high-resolution satellite total column $CO_2$ mole fraction ($XCO_2$) observations from the OCO-2 NASA-JPL mission (the v11 dataset). The OCO-2 satellite carries high-resolution spectrometers that return high-precision measurements of reflected sunlight received within the $CO_2$ and $O_2$ bands in the short-wave infrared spectrum (Crisp et al., 2012) and flies on a 705 km sun-synchronous orbit with a 16-day (233 orbits) ground track repeat cycle. The nominal footprint of the OCO-2 ground pixels is 1.29 × 2.25 $km^2$ (across × along track) at nadir, with a cross-track swath width of about 10 km. We only consider “good” retrievals as identified by the $XCO_2$ quality flag of the product.

Although the biases in OCO-2 over the ocean acquired in glint mode have been substantially reduced since the initial version 7 (O'Dell et al., 2018), Chevallier et al. (2019) claimed that the assimilation of OCO-2 ocean observations still produced unrealistic results in their global atmospheric inversions. Consequently, they are not considered in this study. After this selection, all individual observations are assimilated and compared to their corresponding horizontal grid-cells in CHIMERE (i.e. to the CHIMERE $CO_2$ vertical column in this horizontal grid cell), defined for a given observation as that containing the centre of the ground projection of the OCO-2 pixel at the observation time: there is no aggregation of the observations at the model resolution. As described in Section 3.1.2, the CAMS global $CO_2$ inversions are used to complement the vertical columns of $CO_2$ above the top boundary of CHIMERE when comparing the model to $XCO_2$ observations. To make suitable comparisons between simulations and satellite observations, the vertical profiles of $CO_2$ mole fraction in the corresponding atmospheric columns of the model simulations are first interpolated on the satellite $CO_2$ retrieval levels (with a vertical mass-conserving interpolation on pressure levels). Then, the appropriate simulated $XCO_2$ values are computed using both the OCO-2 averaging kernels and prior estimates provided in the OCO-2 retrieval product. As an example, the average of the OCO-2 observations for the month of June 2019 is presented



This project has received funding from the European Union’s Horizon Europe research and innovation programme under grant agreement No 101081395

in Figure 1a while the average of the simulated $XCO_2$ values activating the CO atmospheric source of $CO_2$ corresponding to these observations are presented in Figure 1b.

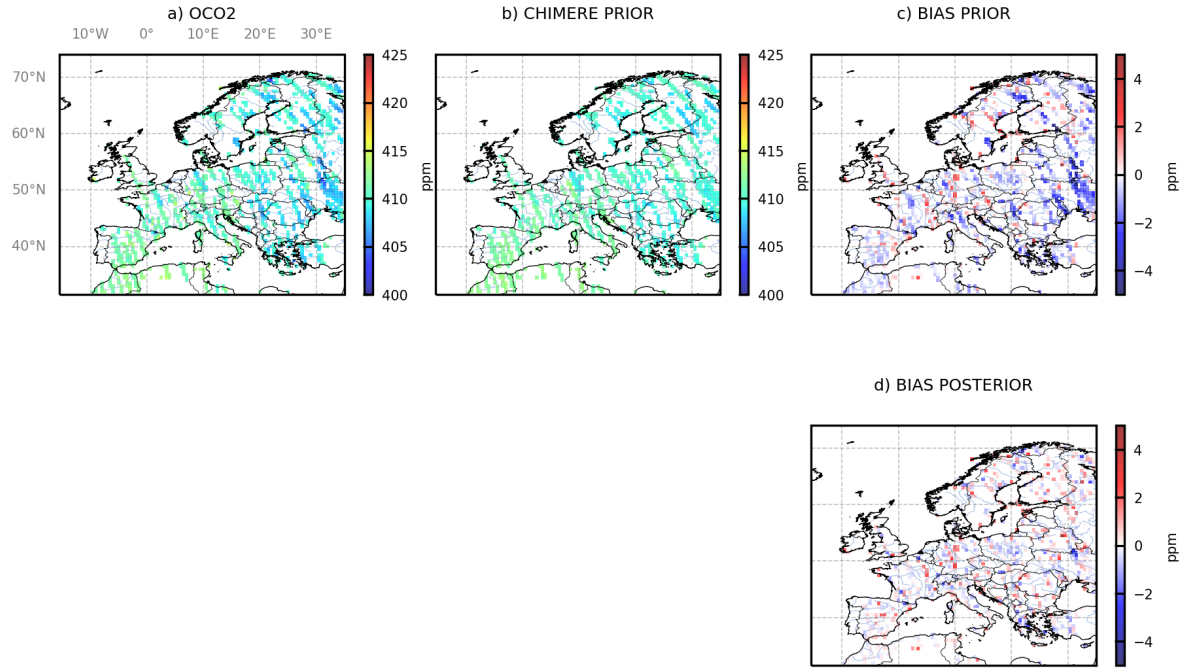


**Figure 1**. Comparison between the OCO-2 $XCO_2$ observations and the corresponding CHIMERE $XCO_2$ simulations activating the CO atmospheric source of $CO_2$ for the month of June 2019: averages over the month of the $XCO_2$ values per grid cell of the model (observations, prior and posterior simulations, and differences), in ppm.

## 1.6. Experiments

The different simulations or inversions for the year 2019 or for the month of June 2019 performed in this study, using ORCHIDEE CRUERA as NEE prior inventory and using OCO-2 satellite observations, are respectively presented in Table 1 and in Table 2.

**Table 1**. Description of the simulations performed in this study for the year 2019.

| Name | Experiment | Chemistry CO-CO2 |
|---|---|---|
| FWD-ref | Forward simulation | no |
| FWD-CO/CO2 | Forward simulation | yes |

**Table 2**. Description of the inversions performed in this study for the month of June 2019.

| Name | Experiment | Control of the initial conditions | Control of the lateral conditions | Chemistry CO-CO2 |
|---|---|---|---|---|
| INV-ref | inversion | yes | yes | no |
| INV-CO/CO2 | inversion | yes | yes | yes |



This project has received funding from the European Union's Horizon Europe research and innovation programme under grant agreement No 101081395

# 2. Results

## 2.1. Computational cost

The computational cost of the different experiments performed in this study are presented in Table 3. Forward simulations have been performed for the entire year 2019. Inversions have been performed for the month of June 2019.

While an inversion takes only 10 hours with 10 processors when $CO_2$ is considered as a passive tracer, an inversion takes more than 8 days when the CO atmospheric source of $CO_2$ is considered with the MELCHIOR-2 chemistry scheme (Table 3). This computational cost could be reduced in the future by having a highly simplified linear chemical scheme in which CO oxidation to $CO_2$ is a first order process using pre-calculated fields of radical hydroxyl OH. In addition, technical developments on CHIMERE, in particular by porting the code to GPU-compatible environment, are currently in progress to allow future series of reference long-term inversions in D3.4. It would also help to perform inversions considering the $CO/CO_2$ chemistry, if relevant. However, further optimizations over the requested memory are still needed to accommodate carrying out adjoint simulations.

**Table 3**. Description of the experiments performed in this study and associated computational cost.

| Experiment | Period | Activating the CO atmospheric source of $CO_2$ | Total Computational cost |
|---|---|---|---|
| FWD-ref | Year 2019 | no | 2 hours |
| FWD-CO/CO2 | Year 2019 | yes | 3 days |
| INV-ref | June 2019 | no | 10 hours |
| INV-CO/CO2 | June 2019 | yes | 8 days |

## 2.2. Comparison between simulations of the $CO_2$ mole fractions activating or not the CO atmospheric source of $CO_2$

Prior simulations with and without activating the CO atmospheric source are compared in Figure 2, and result in differences of less than 0.01% in the $CO_2$ simulated concentrations at the surface. The prior simulations with and without activating the CO atmospheric source are also compared to measurements of $CO_2$ mole fraction from the European Obspack compilation of atmospheric carbon dioxide data from ICOS and non-ICOS European ground based continuous measurement stations for the period 1972-2022 called "obspackco2466GLOBALVIEWplusv8.02023-03-30" (ICOS RI et al., 2023). Comparisons between the bias and root mean square (RMS) differences (denoted RMS errors, i.e., RMSE) between the time series of measured and simulated concentrations are show in Tables 4 and 5 and in Figure 3. When taking the hourly assimilated observations of all the stations into account, **the mean monthly biases between simulated versus measured are very similar, whether the CO atmospheric source of $CO_2$ is activated or not, both at the yearly scale (mean bias of 1.23 ppm against 1.24 ppm, Table 4) or at the monthly scale for the month of June 2019** (mean bias of 1.54 ppm against 1.56 ppm, Table 5). The mean monthly RMSE between simulated versus measured $CO_2$, of about 6 ppm at the yearly scale and 4.99 ppm for the month of June 2019, are equal whether the CO atmospheric source of $CO_2$ is activated or not. These similarities in terms of bias and RMSE are seen for all the stations (Figure 3).



This project has received funding from the European Union's Horizon Europe research and innovation programme under grant agreement No 101081395

These first analysis only show a very slight impact of the activation of the CO atmospheric of $CO_2$ on $CO_2$ simulated concentrations at the surface. It also does not show a clear improvement of the comparison with surface measurements.

**Table 4**. Statistics on the performance of the CHIMERE CTM compared to independent surface mole fraction measurements, for the year 2019. Mean prior of determinant coefficient ($r^2$), Root mean squared error (RMSE) and bias, taking into account all the assimilated surface stations.

| Experiment | $r^2$ | RMSE (ppm) | Bias (ppm) |
|---|---|---|---|
| FWD-ref | 0.53 | 5.91 | 0.31 |
| FWD-CO/CO2 | 0.53 | 5.91 | 0.32 |

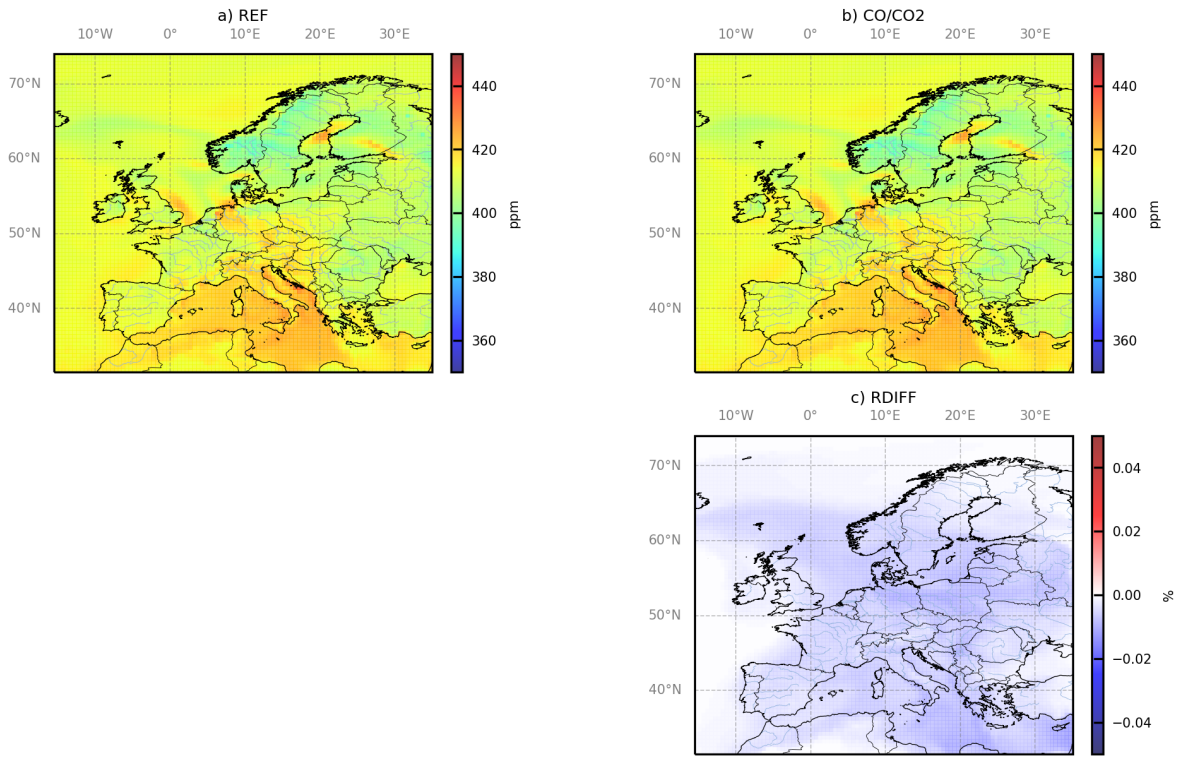


**Figure 2**. CHIMERE $CO_2$ simulated concentrations at the surface, activating the CO atmospheric source of $CO_2$ (b) or not (a), in ppm and c) Relative differences, in %. Illustration for the 15th of June 2019 at 10 am.



This project has received funding from the European Union's Horizon Europe research and innovation programme under grant agreement No 101081395

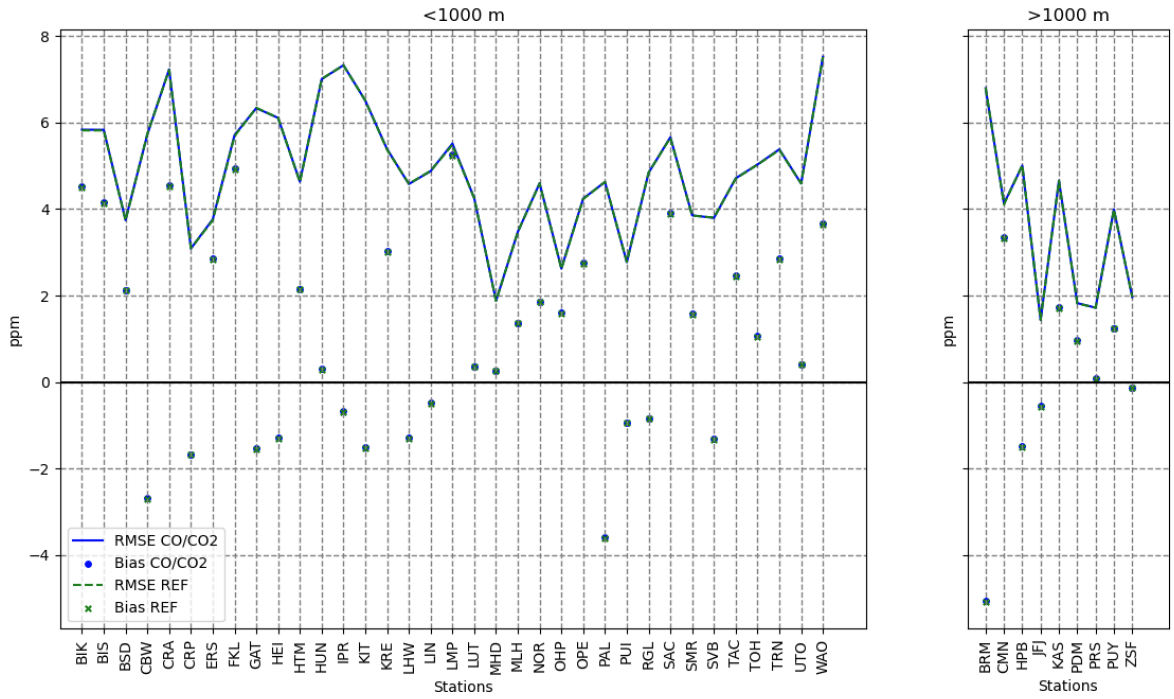


**Figure 3**. Forward simulation activating (blue) or not (green) the CO atmospheric source of $CO_2$ mean bias (dots) and RMSE (solid lines) at observation site with altitude lower (left) and higher (right) than 1000m, in ppm, for the month of June 2019.

### Fit to the assimilated OCO-2 observations

The reduction of the misfits between the simulation and the assimilated observations due to the corrections applied by the CIF-CHIMERE inversions to their prior estimate of the NEE is illustrated in Figure 1d. The prior misfits between these observations and the prior simulation are strongly decreased, with a reduction of the bias reaching about 78% and 77%, respectively with the simulations activating the CO atmospheric source of $CO_2$ or not, in June 2019.

Corrections to the NEE fluxes therefore seem to produce a clear improvement in the fit of simulated mole fractions to the satellite observations. **The bias between the OCO-2 observations and the simulation is reduced in a similar way with the simulations with and without activating the CO atmospheric source of $CO_2$.**

## 2.3. Evaluation of the posterior emissions with independent surface measurements

The evaluation of the NEE posterior fluxes –was made by comparing posterior simulations with independent surface measurements and is illustrated in Figure 4 and in Table 5, which present statistics for all the available stations in June 2019. The corrections applied by the CIF-CHIMERE inversion to the prior estimate of the NEE from the OCO-2 satellite observations mainly result in an improvement of the comparison with surface measurements.

For example, when taking the hourly surface observations of all the stations into account, the increase (from the prior to the posterior simulations) of the monthly $r^2$ coefficient between simulated versus measured $CO_2$ is about 15% whether the CO atmospheric source of $CO_2$ is considered or not (Table 5). The mean biases between simulated versus measured $CO_2$ are also strongly decreased by about 96% whether the CO atmospheric source of $CO_2$ is considered or not (Table 5). **Corrections to the NEE fluxes with a system considering the atmospheric source of $CO_2$** results **in a similar comparison of simulated**



This project has received funding from the European Union's Horizon Europe research and innovation programme under grant agreement No 101081395

**mole fractions with surface measurements as a system not considering the atmospheric source of CO2.**

**Table 5**. Statistics on the performance of the CHIMERE CTM compared to independent surface mole fraction measurements, before and after the inversions, for the month of June 2019. Mean prior and posterior of determinant coefficient ($r^2$), Root mean squared error (RMSE) and bias, considering all the assimilated surface stations.

| | $r^2$ | | RMSE (ppm) | | Bias (ppm) | |
|---|---|---|---|---|---|---|
| **Experiment** | prior | post | prior | post | prior | post |
| **INV-ref** | 0.21 | 0.25 | 4.85 | 5.08 | 0.79 | -0.17 |
| **INV-CO/$CO_2$** | 0.21 | 0.25 | 4.85 | 5.08 | 0.78 | -0.18 |

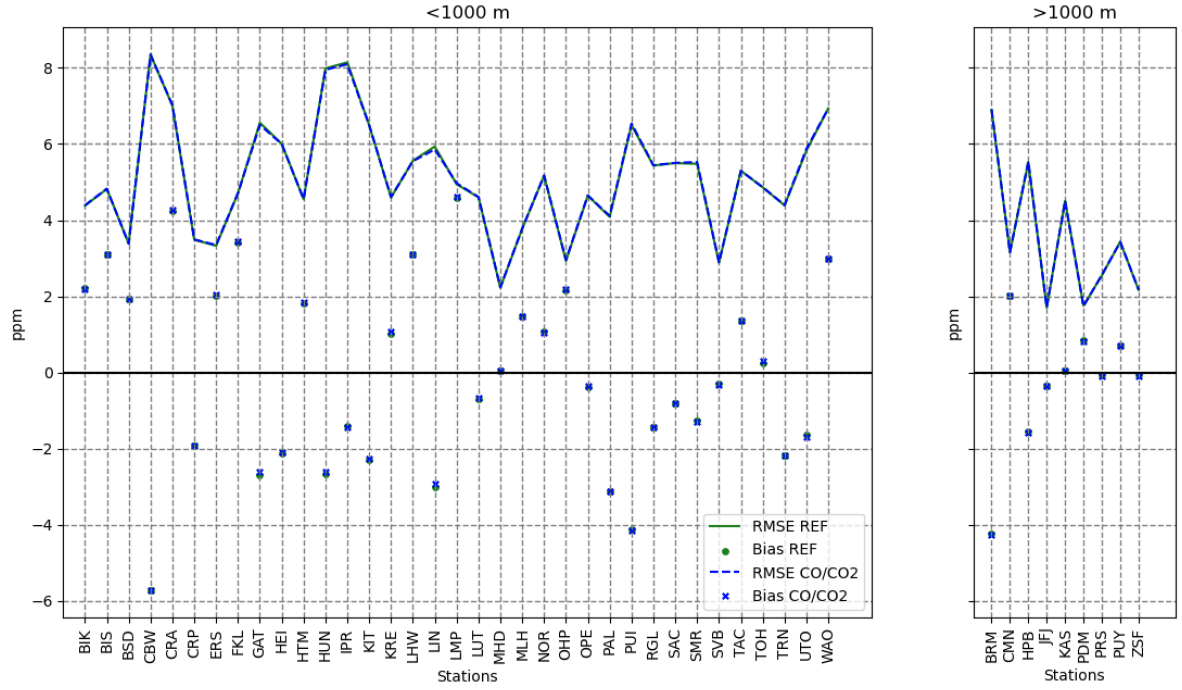


**Figure 4.** Evaluation of the posterior simulation activating the CO atmospheric source of CO2 (blue) or not (green) mean bias (dots) and RMSE (solid lines) at independent surface measurements, in ppm, for the month of June 2019.

## 2.4. EU27+3 NEE budget and spatial variability of the corrections applied to the prior terrestrial ecosystem fluxes from surface observations

Both the inversions, considering the CO atmospheric source of $CO_2$ or not, result in a NEE budget of about -0.29 PgC for the EU-27+3 area (including United Kingdom, Switzerland and Norway in addition to EU-27) from the ORCHIDEE CRUERA prior estimates of about -0.23 PgC, for the month of June 2019.

Figure 5 presents maps of the corrections provided by the inversions to the ORCHIDEE CRUERA prior estimates when assimilating OCO-2 satellite observations in June 2019, whether the CO atmospheric source of $CO_2$ is considered or not. The patterns of the corrections are very similar, with differences not exceeding 5%, whether considering the CO atmospheric source of $CO_2$ or not. Considering the CO



This project has received funding from the European Union's Horizon Europe research and innovation programme under grant agreement No 101081395

atmospheric source of $CO_2$ or not, therefore, does not seem to have an impact on the spatial corrections applied to the prior terrestrial ecosystem fluxes, at least at the monthly scale in summer.

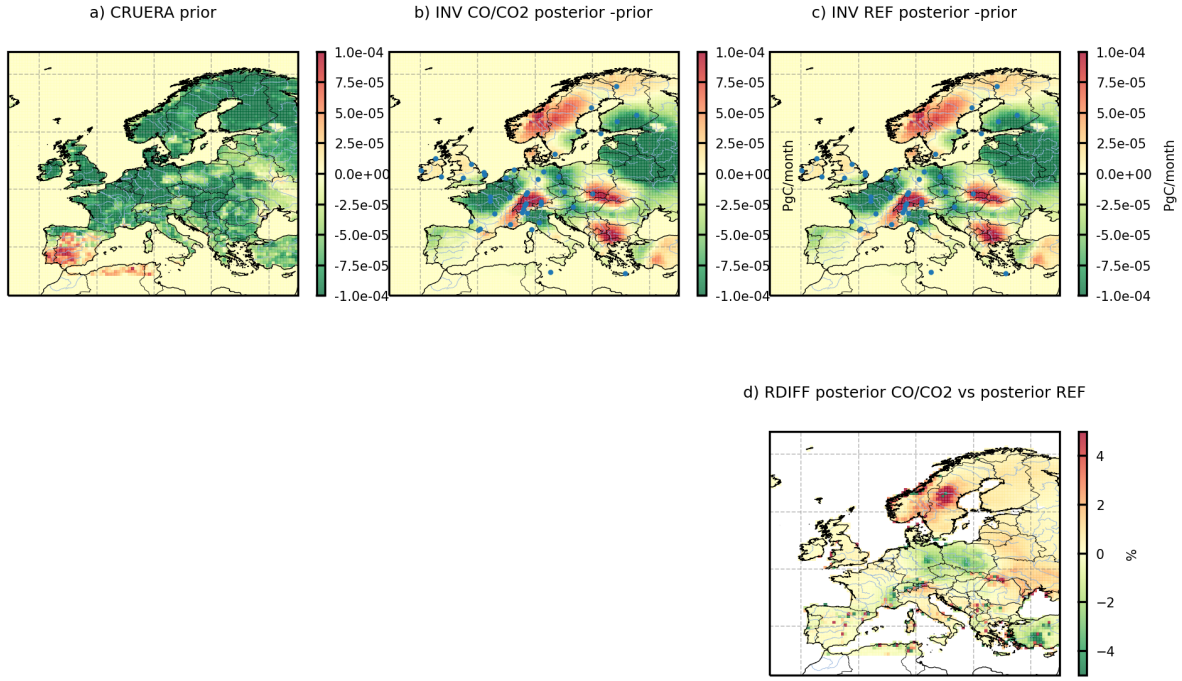


**Figure 5.** a) ORCHIDEE CRUERA prior estimates and maps of the corrections provided by the inversions to the prior when assimilating OCO-2 satellite observations, considering the CO atmospheric source of $CO_2$ (b) or not (c), in PgC/month, in June 2019. d) Relative differences between the posterior NEE fluxes considering the CO atmospheric source of $CO_2$ or not. Blue circles indicate the location of the surface stations used for the evaluation of the NEE posterior estimates.

## Conclusions

Several conclusions can be made:

- The computational cost of the inversions is much higher when the CO atmospheric source of $CO_2$ is activated versus not activated. This computational cost could be reduced in the future by using pre-calculated OH and treating CO oxidation to $CO_2$ as first order process, or by porting the CHIMERE code to GPU-compatible environment.
- The mean monthly biases between simulated and measured CO2 mole fractions are very similar both at the yearly scale and at the monthly scale for the month of June 2019 whether the CO atmospheric source of $CO_2$ is activated or not.
- The spatial corrections applied to the prior terrestrial ecosystem fluxes are similar in June 2019 when the posterior estimates at the 0.5° spatial resolution identify a $CO_2$ peak uptake, whether the CO atmospheric source of $CO_2$ is activated or not.

At this stage, we therefore recommend not considering the CO atmospheric source of $CO_2$ for the inversions of $CO_2$ land ecosystem fluxes.



This project has received funding from the European Union's Horizon Europe research and innovation programme under grant agreement No 101081395

## References

Berchet, A., Sollum, E., Thompson, R. L., Pison, I., Thanwerdas, J., Broquet, G., Chevallier, F., Aalto, T., Berchet, A., Bergamaschi, P., Brunner, D., Engelen, R., Fortems-Cheiney, A., Gerbig, C., Groot Zwaaftink, C. D., Haussaire, J.-M., Henne, S., Houweling, S., Karstens, U., Kutsch, W. L., Luijkx, I. T., Monteil, G., Palmer, P. I., van Peet, J. C. A., Peters, W., Peylin, P., Potier, E., Rödenbeck, C., Saunois, M., Scholze, M., Tsuruta, A., and Zhao, Y.: The Community Inversion Framework v1.0: a unified system for atmospheric inversion studies, Geoscientific Model Development, 14, 5331–5354, https://doi.org/10.5194/gmd-14-5331-2021, 2021.

Broquet, G., Chevallier, F., Rayner, P., Aulagnier, C., Pison, I., Ramonet, M., Schmidt, M., Vermeulen, A., and Ciais, P.: A European summertime CO 2 biogenic flux inversion at mesoscale from continuous in situ mixing ratio measurements, Journal of Geophysical Research: Atmospheres, 116, D23 303 1–22, https://doi.org/10.1029/2011JD016202, 2011.

Broquet, G., Chevallier, F., Bréon, F.-M., Kadygrov, N., Alemanno, M., Apadula, F., Hammer, S., Haszpra, L., Meinhardt, F., Morguí, J. A., Necki, J., Piacentino, S., Ramonet, M., Schmidt, M., Thompson, R. L., Vermeulen, A. T., Yver, C., and Ciais, P.: Regional inversion of CO2 ecosystem fluxes from atmospheric measurements: reliability of the uncertainty estimates, Atmospheric Chemistry and Physics, 13,175 9039–9056, https://doi.org/10.5194/acp-13-9039-2013, 2013.

Chevallier, F.: Fluxes of Carbon Dioxide from Managed Ecosystems Estimated by National Inventories Compared to Atmospheric Inverse Modeling, Geophysical Research Letters, 48, e2021GL093 565, https://doi.org/https://doi.org/10.1029/2021GL093565, e2021GL093565 2021GL093565, 2021.

Chevallier, F., Fisher, M., Peylin, P., Serrar, S., Bousquet, P., Bréon, F.-M., Chédin, A., and Ciais, P.: Inferring CO2 sources and sinks from satellite observations: Method and application to TOVS data, Journal of Geophysical Research: Atmospheres, 110, https://doi.org/https://doi.org/10.1029/2005JD006390, 2005.

Chevallier, F., et al. (2010), $CO_2$ surface fluxes at grid point scale estimated from a global 21 year reanalysis of atmospheric measurements, *J. Geophys. Res.*, 115, D21307, doi:10.1029/2010JD013887.

Chevallier, F., Remaud, M., O'Dell, C. W., Baker, D., Peylin, P., and Cozic, A.: Objective evaluation of surface- and satellite-driven carbon dioxide atmospheric inversions, Atmospheric Chemistry and Physics, 19, 14 233–14 251, https://doi.org/10.5194/acp-19-14233-2019, 2019.

Denier van der Gon, H., Hendriks, C., Kuenen, J., Segers, A., and Visschedijk, A.: TNO Report Description of current temporal emission patterns and sensitivity of predicted AQ for temporal emission patterns EU FP7 MACC deliverable report DD – EM IS1.3, Tech. rep., 2019.

Fortems-Cheiney, A., Pison, I., Broquet, G., Dufour, G., Berchet, A., Potier, E., Coman, A., Siour, G., and Costantino, L.: Variational regional inverse modeling of reactive species emissions with PYVAR-CHIMERE-v2019, Geoscientific Model Development, 14, 2939–2957, https://doi.org/10.5194/gmd-14-2939-2021, 2021b.

Friedlingstein, P., O'Sullivan, M., Jones, M. W., Andrew, R. M., Gregor, L., Hauck, J., Le Quéré, C., Luijkx, I. T., Olsen, A., Peters, G. P., Peters, W., Pongratz, J., Schwingshackl, C., Sitch, S., Canadell, J. G., Ciais, P., Jackson, R. B., Alin, S. R., Alkama, R., Arneth, A., Arora, V. K., Bates, N. R., Becker, M., Bellouin, N., Bittig, H. C., Bopp, L., Chevallier, F., Chini, L. P., Cronin, M., Evans, W., Falk, S., Feely, R. A., Gasser, T., Gehlen, M., Gkritzalis, T., Gloege, L., Grassi, G., Gruber, N., Gürses, O.,Harris, I., Hefner, M., Houghton, R. A., Hurtt, G. C., Iida, Y., Ilyina, T., Jain, A. K., Jersild, A., Kadono, K., Kato, E., Kennedy, D., Klein



This project has received funding from the European Union's Horizon Europe research and innovation programme under grant agreement No 101081395

Goldewijk, K., Knauer, J., Korsbakken, J. I., Landschützer, P., Lefèvre, N., Lindsay, K., Liu, J., Liu, Z., Marland, G., Mayot, N., McGrath, M. J., Metzl, N., Monacci, N. M., Munro, D. R., Nakaoka, S.-I., Niwa, Y., O'Brien, K., Ono, T., Palmer, P. I., Pan, N., Pierrot, D., Pocock, K., Poulter, B., Resplandy, L., Robertson, E., Rödenbeck, C., Rodriguez, C., Rosan, T. M., Schwinger, J., Séférian, R., Shutler, J. D., Skjelvan, I., Steinhoff, T., Sun, Q., Sutton, A. J., Sweeney, C., Takao, S., Tanhua, T., Tans, P. P., Tian, X., Tian, H., Tilbrook, B., Tsujino, H., Tubiello, F., van der Werf, G. R., Walker, A. P., Wanninkhof, R., Whitehead, C., Willstrand Wranne, A., Wright, R., Yuan, W., Yue, C., Yue, X., Zaehle, S., Zeng, J., and Zheng, B.: Global Carbon Budget 2022, Earth System Science Data, 14, 4811–4900, https://doi.org/10.5194/essd-14-4811-2022, 2022.

Koch, F.-T., Gerbig, C., 2023. European anthropogenic CO2 emissions based on EDGARv4.3 and BP statistics 2023 for 2005-2022. https://doi.org/10.18160/RFJD-QV8J

Gilbert, J. and Lemaréchal, C.: Some numerical experiments with variable storage quasi-Newton algorithms, Math. Program., 45, 407–435, https://doi.org/10.1007/BF01589113, 1989.

ICOS RI, Bergamaschi, P., Colomb, A., De Mazière, M., Emmenegger, L., Kubistin, D., Lehner, I., Lehtinen, K., Lund Myhre, C., Marek, M., Platt, S. M., Plaß-Dülmer, C., Schmidt, M., Apadula, F., Arnold, S., Blanc, P.-E., Brunner, D., Chen, H., Chmura, L., Conil, S., Couret, C., Cristofanelli, P., Delmotte, M., Forster, G., Frumau, A., Gheusi, F., Hammer, S., Haszpra, L., Heliasz, M., Henne, S., Hoheisel, A., Kneuer, T., Laurila, T., Leskinen, A., Leuenberger, M., Levin, I., Lindauer, M., Lopez, M., Lunder, C., Mammarella, I., Manca, G., Manning, A., Marklund, P., Martin, D., Meinhardt, F., Müller-Williams, J., Necki, J., O'Doherty, S., Ottosson-Löfvenius, M., Philippon, C., Piacentino, S., Pitt, J., Ramonet, M., Rivas-Soriano, P., Scheeren, B., Schumacher, M., Sha, M. K., Spain, G., Steinbacher, M., Sørensen, L. L., Vermeulen, A., Vítková, G., Xueref-Remy, I., di Sarra, A., Conen, F., Kazan, V., Roulet, Y.-A., Biermann, T., Heltai, D., Hensen, A., Hermansen, O., Komínková, K., Laurent, O., Levula, J., Pichon, J.-M., Smith, P., Stanley, K., Trisolino, P., ICOS Carbon Portal, ICOS Atmosphere Thematic Centre, ICOS Flask And Calibration Laboratory, and ICOS Central Radiocarbon Laboratory: European Obspack compilation of atmospheric carbon dioxide data from ICOS and non-ICOS European stations for the period 1972-2023; obspackco2466GLOBALV IEW plusv 8.02023 – 04 – 26, https: //doi.org/10.18160/CEC4 – CAGK, 2023.

Janssens-Maenhout, G., Crippa, M., Guizzardi, D., Muntean, M., Schaaf, E., Dentener, F., Bergamaschi, P., Pagliari, V., Olivier, J. G. J., Peters, J. A. H. W., van Aardenne, J. A., Monni, S., Doering, U., Petrescu, A. M. R., Solazzo, E., and Oreggioni, G. D.: EDGAR v4.3.2 Global Atlas of the three major greenhouse gas emissions for the period 1970–2012, Earth System Science Data, 11, 959–1002, https://doi.org/10.5194/essd-11-959-2019, 2019.

Jung, M., Schwalm, C., Migliavacca, M., Walther, S., Camps-Valls, G., Koirala, S., Anthoni, P., Besnard, S., Bodesheim, P., Carvalhais, N., Chevallier, F., Gans, F., Goll, D. S., Haverd, V., Köhler, P., Ichii, K., Jain, A. K., Liu, J., Lombardozzi, D., Nabel, J. E. M. S., Nelson, J. A., O'Sullivan, M., Pallandt, M., Papale, D., Peters, W., Pongratz, J., Rödenbeck, C., Sitch, S., Tramontana, G., Walker, A., Weber, U., and Reichstein, M.: Scaling carbon fluxes from eddy covariance sites to globe: synthesis and evaluation of the FLUXCOM approach, Biogeosciences, 17, 1343–1365, https://doi.org/10.5194/bg-17-1343-2020, 2020.

Kountouris, P., Gerbig, C., Totsche, K.-U., Dolman, A. J., Meesters, A. G. C. A., Broquet, G., Maignan, F., Gioli, B., Montagnani, L., and Helfter, C.: An objective prior error quantification for regional atmospheric inverse applications, Biogeosciences, 12, 7403–7421, https://doi.org/10.5194/bg-12-7403-2015, 2015.



This project has received funding from the European Union's Horizon Europe research and innovation programme under grant agreement No 101081395

Krinner, G., Viovy, N., de Noblet-Ducoudré, N., Ogée, J., Polcher, J., Friedlingstein, P., Ciais, P., Sitch, S., and Prentice, I. C.: A dynamic global vegetation model for studies of the coupled atmosphere-biosphere system, Global Biogeochemical Cycles, 19, https://doi.org/https://doi.org/10.1029/2003GB002199, 2005.

Mahadevan, P., Wofsy, S. C., Matross, D. M., Xiao, X., Dunn, A. L., Lin, J. C., Gerbig, C., Munger, J. W., Chow, V. Y., and Gottlieb, E. W.: A satellite-based biosphere parameterization for net ecosystem CO2 exchange: Vegetation Photosynthesis and Respiration Model (VPRM), Global Biogeochemical Cycles, 22, https://doi.org/https://doi.org/10.1029/2006GB002735, 2008.

Mailler, S., Menut, L., Khvorostyanov, D., Valari, M., Couvidat, F., Siour, G., Turquety, S., Briant, R., Tuccella, P., Bessagnet, B., Colette, A., Létinois, L., Markakis, K., and Meleux, F.: CHIMERE-2017: from urban to hemispheric chemistry-transport modeling, Geoscientific Model Development, 10, 2397–2423, https://doi.org/10.5194/gmd-10-2397-2017, 2017.

McGrath, M. J., Petrescu, A. M. R., Peylin, P., Andrew, R. M., Matthews, B., Dentener, F., Balkovi˘c, J., Bastrikov, V., Becker, M., Broquet, G., Ciais, P., Fortems, A., Ganzenmüller, R., Grassi, G., Harris, I., Jones, M., Knauer, J., Kuhnert, M., Monteil, G., Munassar, S., Palmer, P. I., Peters, G. P., Qiu, C., Schelhaas, M.-J., Tarasova, O., Vizzarri, M., Winkler, K., Balsamo, G., Berchet, A., Briggs, P., Brockmann, P., Chevallier, F., Conchedda, G., Crippa, M., Dellaert, S., Denier van der Gon, H. A. C., Filipek, S., Friedlingstein, P., Fuchs, R., Gauss, M., Gerbig, C., Guizzardi, D., Günther, D., Houghton, R. A., Janssens-Maenhout, G., Lauerwald, R., Lerink, B., Luijkx, I. T., Moulas, G., Muntean, M., Nabuurs, G.-J., Paquirissamy, A., Perugini, L., Peters, W., Pilli, R., Pongratz, J., Regnier, P., Scholze, M., Serengil, Y., Smith, P., Solazzo, E., Thompson, R. L., Tubiello, F. N., Vesala, T., and Walther, S.: The consolidated European synthesis of CO2 emissions and removals for EU27 and UK: 1990–2020, Earth System Science Data Discussions, 2023, 1–123, https://doi.org/10.5194/essd-2022-412, 2023.

Menut, L., Bessagnet, B., Khvorostyanov, D., Beekmann, M., Blond, N., Colette, A., Coll, I., Curci, G., Foret, G., Hodzic, A., Mailler, S., Meleux, F., Monge, J.-L., Pison, I., Siour, G., Turquety, S., Valari, M., Vautard, R., and Vivanco, M. G. : CHIMERE 2013: a model for regional atmospheric composition modelling, Geoscientific Model Development, 6, 981–1028, https://doi.org/10.5194/gmd-6-981-2013, 2013.

Monteil, G., Broquet, G., Scholze, M., Lang, M., Karstens, U., Gerbig, C., Koch, F.-T., Smith, N. E., Thompson, R. L., Luijkx, I. T., White, E., Meesters, A., Ciais, P., Ganesan, A. L., Manning, A., Mischurow, M., Peters, W., Peylin, P., Tarniewicz, J., Rigby, M., Rödenbeck, C., Vermeulen, A., and Walton, E. M.: The regional European atmospheric transport inversion comparison, EUROCOM: first results on European-wide terrestrial carbon fluxes for the period 2006–2015, Atmospheric Chemistry and Physics, 20, 12 063–12 091, https://doi.org/10.5194/acp-20-12063-2020, 2020.

Munassar, S., Rödenbeck, C., Koch, F.-T., Totsche, K. U., Gałkowski, M., Walther, S., and Gerbig, C.: Net ecosystem exchange (NEE) estimates 2006–2019 over Europe from a pre-operational ensemble-inversion system, Atmospheric Chemistry and Physics, 22, 7875–7892, https://doi.org/10.5194/acp-22-7875-2022, 2022.

O'Dell, C. W., Eldering, A., Wennberg, P. O., Crisp, D., Gunson, M. R., Fisher, B., Frankenberg, C., Kiel, M., Lindqvist, H., Mandrake, L., Merrelli, A., Natraj, V., Nelson, R. R., Osterman, G. B., Payne, V. H., Taylor, T. E., Wunch, D., Drouin, B. J., Oyafuso, F., Chang, A., McDuffie, J., Smyth, M., Baker, D. F., Basu, S., Chevallier, F., Crowell, S. M. R., Feng, L., Palmer, P. I., Dubey, M., García, O. E., Griffith, D. W. T., Hase, F., Iraci, L. T., Kivi, R., Morino, I., Notholt, J., Ohyama, H., Petri, C., Roehl, C. M., Sha, M. K., Strong, K., Sussmann, R., Te, Y., Uchino, O., and Velazco, V. A.: Improved retrievals of carbon dioxide



This project has received funding from the European Union's Horizon Europe research and innovation programme under grant agreement No 101081395

from Orbiting Carbon Observatory-2 with the version 8 ACOS algorithm, Atmospheric Measurement Techniques, 11, 6539–6576, https://doi.org/10.5194/amt-11-6539-2018, 2018.

Petrescu, A. M. R., McGrath, M. J., Andrew, R. M., Peylin, P., Peters, G. P., Ciais, P., Broquet, G., Tubiello, F. N., Gerbig, C., Pongratz, J., Janssens-Maenhout, G., Grassi, G., Nabuurs, G.-J., Regnier, P., Lauerwald, R., Kuhnert, M., Balkovič, J., Schelhaas, M.-J., Denier van der Gon, H. A. C., Solazzo, E., Qiu, C., Pilli, R., Konovalov, I. B., Houghton, R. A., Günther, D., Perugini, L., Crippa, M., Ganzenmüller, R., Luijkx, I. T., Smith, P., Munassar, S., Thompson, R. L., Conchedda, G., Monteil, G., Scholze, M., Karstens, U., Brockmann, P., and Dolman, A. J.: The consolidated European synthesis of $CO_2$ emissions and removals for the European Union and United Kingdom: 1990–2018, Earth Syst. Sci. Data, 13, 2363–2406, https://doi.org/10.5194/essd-13-2363-2021, 2021.

Rödenbeck, C., Bakker, D. C. E., Metzl, N., Olsen, A., Sabine, C., Cassar, N., Reum, F., Keeling, R. F., and Heimann, M.: Interannual sea–air CO2 flux variability from an observation-driven ocean mixed-layer scheme, Biogeosciences, 11, 4599– 4613, https://doi.org/10.5194/bg-11-4599-2014, 2014.

Sitch, S., Friedlingstein, P., Gruber, N., Jones, S. D., Murray-Tortarolo, G., Ahlström, A., Doney, S. C., Graven, H., Heinze, C., Huntingford, C., Levis, S., Levy, P. E., Lomas, M., Poulter, B., Viovy, N., Zaehle, S., Zeng, N., Arneth, A., Bonan, G., Bopp, L., Canadell, J. G., Chevallier, F., Ciais, P., Ellis, R., Gloor, M., Peylin, P., Piao, S. L., Le Quéré, C., Smith, B., Zhu, Z., and Myneni, R.: Recent trends and drivers of regional sources and sinks of carbon dioxide, Biogeosciences, 12, 653–679, https://doi.org/10.5194/bg-12-653-2015, 2015.

Steinbach, J., Gerbig, C., Rödenbeck, C., Karstens, U., Minejima, C., and Mukai, H.: The CO2 release and Oxygen uptake from Fossil Fuel Emission Estimate (COFFEE) dataset: effects from varying oxidative ratios, Atmosph eric Chemistry and Physics, 11, 6855–6870, https://doi.org/10.5194/acp-11-6855-2011.

Thompson, R. L., Broquet, G., Gerbig, C., Koch, T., Lang, M., Monteil, G., Munassar, S., Nickless, A., Scholze, M., Ramonet, M., Karstens, U., van Schaik, E., Wu, Z., and Rödenbeck, C.: Changes in net ecosystem exchange over Europe during the 2018 drought based on atmospheric observations, Philos. T. R. Soc. B, 375, 20190512, 2020.



This project has received funding from the European Union's Horizon Europe research and innovation programme under grant agreement No 101081395

https://eyeclima.eu

BRUSSELS, 22.04.2025

*Funded by the European Union. Views and opinions expressed are however those of the author(s) only and do not necessarily reflect those of the European Union. Neither the European Union nor the granting authority can be held responsible for them.*

This project has received funding from the European Union's Horizon Europe research and innovation programme under grant agreement No 101081395